MILLIMETER ARRAY
MEMO NO. 110

HOMOLOGOUS OFFSET ANTENNA CONCEPT FOR THE MILLIMETER ARRAY PROJECT

Jingquan Cheng

March 22, 1994

ABSTRACT

A major obstacle in meeting the requirements for the mmA antennas is the gravitationally induced deformations. A new antenna configuration, consisting of an offset reflector combined with a slant axis mounting, has been investigated. With this combination the varying gravitational component is never perpendicular to the antenna surface. This results in gravitational deformations that are substantially smaller than either a conventional antenna or a symmetric slant axis antenna. A preliminary design of an 8-meter offset slant axis antenna produces gravitationally induced deviations from the best fit paraboloid of less than 8 microns in all orientations. Although the major consideration in developing this concept has been the minimization of the gravitational deflections, the design has other substantial advantages, such as greatly reduced blockage and much improved receiver access with reduced (or no) receiver movement as the antenna tracks.

1.0 Introduction.

The Millimeter Array is a high performance instrument for millimeter astronomy. There are strict requirements both statically and dynamically for its antenna structure. Driven by these demanding specifications and considering the construction cost, an unconventional slant axis design was proposed[1],[2]. The design study[3] of the slant axis design shows that the proposed design is more rigid than other types of design and, without the backup structure counterweight, the structure is much lighter. The previously proposed slant axis antenna already satisfied the requirements for the mmA, but the design described here offers several advantages over the previous design. The blockage is greatly reduced and the receiver mounting possibilities and access are greatly improved.

As shown in Figure 1 the indirect blockage of the previously proposed slant axis symmetrical

design is as high as 9%. This relatively high value results from the requirement for a stiff structure for the feed support with a high natural frequency in order to support fast switching. Slightly reducing this feed-leg blockage is possible, but, the stiffness and the natural frequency of the structure will be reduced at the same time and the dynamic performance of the antenna may be affected. As well as reducing antenna efficiency, the blockage will lead to extra ground pickup thereby degrading system temperature[4].

To avoid this aperture blockage problem, an offset antenna design is preferred. However, the backup structure involved for an offset antenna is usually too complicated to handle in the homology design process. For an offset backup structure, there is no overall symmetry in the structural arrangement. This means the implementation of a conventional optimization technique is extremely difficult. For example an 8 m backup structure would suffer gravitational deformations as large as 300 to 500 microns. This is far larger than the rms error required for mmA antennas (the error budget specifies a backup structure error for gravity of only 8 microns[5]). The force distribution of a slant axis configuration results in an offset backup structure that is readily amenable to optimization. In this memo, the offset optics and the slant axis mounting are combined together. In addition with a special double layer space truss design, the offset backup structure has an even smaller surface deformation. This is the first time an offset backup structure has been applied to a highly accurate antenna design without using any active surface control. Structural analysis of a preliminary design shows the offset slant axis design can have a very small gravitational rms error in all pointing directions.

In this memo, Section 2 discusses general homologous design problems, Section 3 discusses the force conditions of a slant axis mounting structure, Section 4 provides a practical mmA antenna design with its optical layout. The details of the antenna backup structure and its shell-like effect are discussed. The same section also provides structural analysis, surface fitting results and other aspects of the antenna. Section 5 lists all the advantages and shortcomings of the present design. Section 6 is the summary and conclusion.

2.0 Homologous design of antenna structure.

The main task in any antenna design is, of course, to optimize the backup structure in order to satisfy the homology requirements. This optimization has two steps[6]. One is the structural analysis, and the other is the best fitting process. The first step may be done by using the standard finite element analysis approach. The structure nodal displacement vector D is related to the applied load vector F by the structural stiffness matrix K, i.e.

$$K D = F$$

If a trial structure is provided, K and F are known, and D can be obtained easily from many available programs. The second step is to fit the surface nodes to a paraboloid. This is a high order fit which converges slowly. For antenna design, this approach is linearized by introducing a set of new variables. The fitting process is to solve a set of linear equations of these variables. These variables may be the vertex displacements in x, y, and z directions, the rotational angles

about x and y axes and the change in the focal length of the paraboloid in the original coordinate system. From the fitting results, the rms surface error is determined. If the rms error is within the required value, the design is successful. But in most cases, the rms error is larger than the required value. Therefore, modification of the structure is required. By modifying the structure, a new D is calculated, and a new rms error is calculated. This process is then be repeated until the rms error is within the design requirement.

However, in practical antenna design, the optimization procedure is very difficult and time consuming, since the magnitude of the difference in the displacements between the deformed surface of a trial structure and its best fitted surface is not an indication of the degree of structural change required in the next design cycle. The relationship between structure parameters and surface displacement pattern is complex and indirect. Any modification of the structural arrangement and members' cross section areas is then made using the designer's judgement. Fixed rules are not available in the design. At the same time, there are many variables which can be used during the trial and error. This also complicates the design procedure. These design variables include: (i) the geometry of the structure (e.g. the coordinates of all nodes in the structure); (ii) the topological description (which of the nodes are connected by members); and (iii) the cross section size and shape of each member.

The above procedure has to be performed both at zenith and horizon pointings for an altazimuth mounting antenna. Fortunately, when the antenna is pointing to the horizon, the system shows a skew mirror symmetry[15] about the plane formed by the axes of the elevation bearings and the parabolic surface. This is to say that the force components of the upper and the lower parts of the structure in their local coordinate system have the same magnitude but opposite sign. The displacement pattern produced shows mainly a linear change with the nodal distances from the central support ring, so the surface tilts due to the gravitational force. The resulting rms error is small. Therefore, most structural optimization is performed when the antenna is at the zenith pointing. At this pointing the gravitational force is mostly normal to the dish surface, so the nodal deflection pattern is very sensitive to any change of the structure. The designer has to avoid any hard points on the surface and must adjust the surface pattern step by step.

For a cyclically symmetric backup structure, the optimization problem can be greatly simplified at the zenith pointing. This is because at this pointing, the gravitational direction is parallel to the axis of the antenna structure. This is a cyclically symmetrical system. For a cyclically symmetrical system, the performance of whole structure can be represented by only one sector of it. Within this sector of the structure, the number of the surface nodes and the number of the structure variables are much less than that of the whole structure. Therefore the optimization is easier. For an 8 m symmetric backup structure, if the number of surface nodes is 96 and there are 12 identical sectors in the structure, then the number of the nodes needed to consider during the optimization at the zenith pointing is only 8.

On the other hand, an offset backup structure will be difficult to optimize as the structure is not cyclically symmetrical. Another difficulty of the offset backup structure exists in distributing the supporting force, which is usually symmetrical about the center of the structure, to the structure

which is unsymmetrical about its center. Because of these difficulties there has until now been no attempt to design a homologous offset backup structure. Most existing offset designs are for smaller antennas or antennas working at longer wavelength. As an illustration of the difficulties in implementing an offset design the 100 m GBT requires active control of no fewer than 2400 points on the surface[7]. This approach is costly and complicated.

3.0 Force distribution of slant axis antenna.

The slant axis mounting arrangement greatly changes the force conditions on the backup structure. In an altazimuth mounting structure, the force applied to the backup structure only has two components in the local coordinate system: one is parallel to the dish axis (F_z) and the other is perpendicular to the plane defined by the axes of the dish and the elevation bearings (F_y), the component along the elevation axis (F_x) is zero(Figure 2-a). The decomposition of the gravitational force at any orientation is:

$$\begin{bmatrix} F_x \\ F_y \\ F_z \end{bmatrix} = \begin{bmatrix} 0 \\ F\cos\alpha \\ F\sin\alpha \end{bmatrix}$$

where α is the elevation angle. The aim of homologous design of the backup structure for an altazimuth antenna is to keep surface nodal positions near to the best fit paraboloid when the gravitational force is applied in both y and z directions. As mentioned above, the optimization in the z direction is more difficult although the system is cyclically symmetrical. However when the force comes from the y direction, the displacement of a surface node is approximately proportional to the distance to the supporting points, resulting in a tilt of the reflecting surface, so easing the fitting and optimization.

For a slant axis antenna, the situation is different. The gravitational force applied has three components in the local coordinate system o-xyz (Figure 2-b). In the o-xyz system, oz direction is along the axis of the slant bearing, ox direction is in the plane of the axes of the paraboloid and the slant bearing, that is the 0-XZ plane of the parent coordinate system, and oy axis is parallel to the OY axis and is perpendicular to the ox axis. The components of the gravitational force at any orientation are:

$$\begin{bmatrix} F_x \\ F_y \\ F_z \end{bmatrix} = \begin{bmatrix} F\sin 45^\circ\cos\theta \\ F\sin 45^\circ\sin\theta \\ F\cos 45^\circ \end{bmatrix}$$

where θ is the rotation angle about slant axis, and 45 degrees is the elevation angle of the slant axis From the equation, it can be seen that the F_z component which is along the slant axis is a constant. It will not change when the antenna is rotating around either slant axis or azimuth axis. Force in this direction is close to the normal of the dish surface, which is always difficult to

optimize. However this constant force component F_z will produce a fixed surface deformation that can be compensated by the panel adjustment, so optimization of the structure in this direction is not necessary. This is the most important feature of the slant axis mounting used in the new design. Therefore only the components F_x and F_y need to be considered during the structural optimization. It should be remembered that a rotation of 180 degrees of the slant axis is required to move the telescope beam from zenith to horizon. The force F_x alone is the only force to be considered when the antenna is pointing at the zenith or horizon and the force F_y is the only force when the antenna is at about 45 degrees in elevation.

The offset structure is symmetrical about the O-XZ plane, and shows a skew symmetry about this plane when the force component F_y is applied. The force components of the upper and the lower parts have the same magnitude but opposite sign in their local mirror symmetrical coordinate system, so design experience suggests that the surface deformations resulting from the F_y component will be amenable to optimization. However the component F_x is different; the structure has no symmetry about the plane normal to the F_x component. The F_x component is not in the direction normal to the reflecting surface. However, further decomposition of this force component results in forces both along the paraboloid surface and normal to the surface. For constant forces acting along a plate surface, the deformations of the surface are linear functions of both the Poisson's ratio and the distances to the supporting points. When a central point support is used, the structural deformation introduced is only a tilt of the surface shape, resulting in no rms error. For a space truss structure, depending on the structure details, there may be surface rms errors caused by the forces acting on the truss surface. The main errors introduced in the backup structure are from the force components which are normal to the surface, and even these components are small in magnitude. Therefore the key to an offset slant axis backup structure design is to eliminate or reduce further the effect of those small force components which are normal to the reflecting surface. The strategy to implement this will be discussed in the next section.

4.0 Practical Design.

The purpose of the practical design is to confirm the discussion of the previous sections and to provide a way to design a homologous offset backup structure used on the slant axis mounting. In this section, the shell effect of the double layer space truss structure is discussed. The practical backup structure will use the shell like property of the space truss to resist surface deformations. In this section the optics formulae for the offset antenna are also introduced. A practical backup structure and its analysis results are provided. This section also mentions other aspects of the proposed offset slant axis antenna. However, the example provided is not a final design; many details have yet to be studied. These include: thermal effects, dynamical performance, wind effect and secondary mirror support structure details. However, the proposed offset design has similar dimensions to the slant axis symmetrical antenna previously studied. It is expected that many aspects will be similar.

4.1 Discussion of the shell effect.

Most antennas use a space truss design to achieve a high stiffness to weight ratio. However, most truss structures used for antennas are irregular in shape. Their performance is unpredictable. Optimization relies on experience. For the offset slant axis backup structure, the main varying gravitational forces are on the reflecting surface; the components normal to it are small. This allows the design of a homologous offset backup structure. The design strategy is still important to reduce the distortion from these forces.

One group of space structures has been widely used in industry, architecture and other fields. This is the double layer space truss structure of a uniform thickness. This type of structure is formed by top, bottom and middle layers of beams. Middle layer members are in diagonal directions. The whole truss structure has a regular repeatable pattern. If the dimensions of the structure are larger than the member length, then its performance may be predicted approximately by the theory of plate analogy. In other words, the space structure will perform to some extent like a thin plate or membrane[9]. The plate analogy gives the equivalent stiffness D_{appro} and the equivalent Poisson's ratio v as:

$$D_{appro}=\frac{A_t A_b}{b(A_t+A_b)}h^2E \qquad v=0$$

where A_t and A_b are the top and bottom layer member areas, b is the spacing between top and bottom members, h is the thickness of the trusses and E is the material Young's modulus.

Following the discussion in the previous section, the rms surface error of this type of double layer truss will be negligible if the force applied is on the truss plane. However the paraboloid surface is curved, so it is not practical to apply this type of truss structure directly. A practical double layer truss structure chosen for the offset backup structure is shown in Figure 3. The structure has a regular repeatable pattern symmetrically arranged about the surface axis. The main members of the truss are in the radial and circumferential directions; its well arranged middle layer members make the structure rigid as a whole. This resists the deformations caused by the slant bearing support points. Incidently, due to the curvatures both in the radial and the circumferential directions, the structure also has a shell-like performance. The forces normal to the surface are nearly uniform in magnitude, which reduces greatly the effect of the deformation caused by forces normal to the surface. This effect will be discussed in the following paragraph.

In the proposed offset slant axis system, the only varying gravitational force components on the backup structure are F_x and F_y. As mentioned before, structural symmetry helps the optimization in the F_y direction. In this paragraph, only the F_x component is discussed in detail. In Figure 4, the F_x component of the gravitational forces has an angle of 45 degrees with the o-r axis in the parent cylindrical coordinate system. Its tangential and radial components on the parabolic surface are:

$$F_{t1}=F_x\cos\theta\ \cos(45-\beta)$$
$$F_{t2}=F_x\sin\theta$$
$$F_r=F_x\cos\theta\ \sin(45-\beta)$$

where tan β=r/2f is the slope of the parabola in the radial planes, F_t and F_r are the force components on the surface and normal to the surface, F_{t1} is the force component on the radial plane and F_{t2} is the component in the circumferential direction. Plate analogy theory and design experience suggest that the force components on the surface results in little or no rms surface errors. The component normal to the surface needs more attention.

A shell structure is a structure which can resist high pressure loads, with relatively little deformation[8]. The conditions of the shell effect are: i) the surface has large radii of curvature in both principle directions; ii) the thickness of the shell is very small compared with these radii of curvature; and iii) there is a pressure applied to the shell. The advantage of the shell effect is to divert the pressure force into stresses on the shell surface. The well-known formula for the shell is[10]:

$$\frac{\sigma_1}{r_1}+\frac{\sigma_2}{r_2}=\frac{P}{h}$$

where σ_1, σ_2 are stresses on the tangential plane of the shell, r_1, r_2 are radii of curvatures in the two principle directions, P is the pressure; and h is the shell thickness (ref. Figure 5). For a space truss structure, a similar situation also exists if the force components normal to the surface applied at all joints are the same in magnitude. In this case, the surface members will undergo extension and compression, and the resulting deformation is small. To obtain the shell effect we require uniform forces normal to the surface at every truss joint. From the previous formulae, the force component normal to the truss surface F_r can be expressed as:

$$F_r=0.707F_x\cos\theta\ \cos\beta\ (1-\frac{r}{2f})$$

where F_x is the weight component of the surface panels the joint supports. The weight of the panel is proportional to the ring area of the parabolic surface S as:

$$S=\frac{1}{2f}\left[r\sqrt{4f^2+r^2}-4f^2\ln\frac{r+\sqrt{4f^2+r^2}}{2f}\right]\Big|_{r_1}^{r_2}$$

For the same panel length, S will increase as r increases. Since θ is ranging from -40 to 40 degrees, the change of cos θ term is smooth. If the last two terms of F_x expression are represented as Q, Q is also a function of r. Fortunately, as r increases, Q will decrease. In the following table, we list the values of S, Q and SQ from r = 1 m to r = 9 m for a parabolic offset

surface with its focal length f = 5 m.

Table 1 The value of S, Q, and SQ

r	1	2	3	4	5	6	7	8	9
S	5.16	10.60	11.32	12.26	13.42	14.76	16.23	17.80	9.53
Q	0.89	0.78	0.66	0.55	0.44	0.34	0.24	0.16	0.07
SQ	4.59	8.26	7.47	6.74	5.89	5.02	3.89	2.85	0.66

In Table 1, the values of S at points r = 1 m and r = 9 m correspond to the area of only one ring of panels, while the joints at other r values will support two adjacent rings of panels. From this table, it can be found that the values of SQ, which are indicative of the forces normal to the truss surface, vary very smoothly for most r values; therefore the double layer backup truss structure does behave like a shell, resulting in an even smaller distortion of the reflecting surface.

4.2 Optics arrangement

The optics of a practical design of the 8 m offset slant axis mmA antenna are shown in Figure 6. The determining factor of the optical arrangement is that the secondary mirror should be on the slant axis which is 45 degrees in elevation. In the figure, two receiver positions are shown. If the receiver is located at the base, there is no movement of the receiver when the antenna is tracking on the sky. However, a third mirror is introduced in this configuration. In the other configuration the receiver is on the altazimuth axis, and only rotates with low speed when the telescope tracks on the sky. The only blockage of the design is a small beam hole in the primary mirror surface.

For the optical design we need to determine the primary focal length. This is done by the consideration of structure balance. If no blockage from the secondary mirror is expected, the 8 m primary mirror surface will have its two ends at r = 1 m and r = 9 m from paraboloid vertex. Since the slant angle is 45 degrees, the intersection of the slant axis and the parabolic surface is at a location where r is about the same as the focal length. For f < 4.5 m, the ratio of the two parts divided by the slant axis is about 3 : 5. For f > 5.5 m, the ratio of the two parts will be about 4 : 4 or more. The ratio of 3 : 5 or less will produce imbalance in the backup structure as the far side of the antenna is wider than the inner side. Also considering the weight of the secondary mirror supporting structure, a ratio of 4 : 4 will also cause inbalance of the structure (the weight of the secondary mirror support is not small), so the focal length in the proposed design is chosen as f = 5 m.

The optics of the antenna are straightforward. The primary mirror is an offset paraboloid and the secondary mirror is a hyperboloid. Figure 7 gives the projected views of the primary and

secondary mirrors. The projected view shows there is no aperture blockage by the secondary mirror and its supporting structure. The optical parameters chosen for the design are:

primary focal length	5 m
Equivalent primary focal ratio	0.28.
Distance from the primary vertex to the mirror edge	9 m
System focal ratio	12
Location of third mirror from the vertex	r = 5.25 m z = -0.25 m

The equation of the primary mirror in the primary spherical coordinate system (aligned with the x_p, y, z_p coordinates of Figure 7) is[11]:

$$r = \frac{2f}{1 + \cos\theta_p}$$

where f= 5 m. If the secondary spherical coordinate system (aligned with x_s, y, z_s of Figure 7) are used, the equation becomes:

$$r = \frac{2f}{1 + \cos\theta\cos\theta_o - \sin\theta\sin\theta_o\cos\phi}$$

Referring to Figure 8, the equation for the hyperboloid secondary mirror surface is given by the equation:

$$|r_1| - |r_2| = b$$

The equation for the hyperboloid surface in terms of θ_1 is:

$$r_1 = \frac{c}{2}\,\frac{(1-\delta^2)}{\delta + \cos\theta_1}$$

where δ = b/c, b and c are determined from the system focal ratio and secondary mirror magnification factor. The shape of the secondary mirror is a revolution about the slant axis.

4.3. The analysis results.

Figure 9 is a perspective view of the design. The primary mirror surface of the antenna is formed by 118 regular fan shaped panels and 14 special edge panels. The shaped panels are used for avoiding the edge discontinuity of the primary mirror. The panels are located in 10 rings. The

largest dimension of all panels is about 1 m. The panel support structure is a double layer shell-like space truss (ref. Figure 3). The thickness of the truss is about 0.3 m. The surface nodal number is 149. All the members of the double layer truss are small carbon fiber reinforced plastic tubes. The diameter of these tubes is 1 inch. The members of the truss are arranged to make the structure have equal stiffness parallel to the circumference of the parent paraboloid. The truss has a repeated pattern in both radial and tangential directions. This eases the manufacture and lowers the cost. Between the double layer truss structure and the slant bearing disk, there is another third layer of truss. This truss has the shape of horseshoe. The supporting members under the double layer truss have larger sectional areas: two section sizes are used in the model; these are 3 inches and 5 inches. The supporting disk on the slant bearing has a diameter of 4 m. The analysis weight of the backup structure including the weight of the panels is 2.0 tons without secondary mirror supporting structure. In the model, the weight of joints is not included. The final backup structure will weigh more and the rms will be slightly higher when the weight of joints is added.

The structural analysis has been performed when the gravitational component is in the x and y directions of the local coordinate system. Since the maximum gravitational component in these directions is only 0.707 of the total gravitational force applied, a factor of 0.707 is used in the structural analysis. The structural analysis is performed by the Nastran program. After the analysis, parabolic surface fitting is carried out. The fitting program used was developed by the author and is a minimization of the nodal distances from the best fitted paraboloid. The result is therefore conservative compared with the half-pathlength minimization. The whole optimization is straightforward. The main change on the structure is to make the bottom support points on the far end from the vertex symmetrical around the parent surface axis.

If the x- component of gravitational force is applied, the maximum surface displacement has an absolute value of only about 40 microns, and the rms error of the surface after fitting for the first model is only 6.3 microns. The rms error for the second model is as small as 3.1 microns. In the parent coordinate system, the vertex displacement of the best fit paraboloid in mm is (- 0.15, - 0.02, 0.01), the rotational angles in x and y direction is 0.000002 and 0.000012 radians, and the new focal length is 4.9998 m.

When the y- component of the gravitational force is applied, the rms error change for different structure arrangements is small, ranging from 7.9 microns to 10 microns. The resulting design of the second model has an rms error of 7.9 microns. In this case the vertex displacement in mm is (0.02, 0.57, -0.00) and the rotational angles in x and y directions are 0.00006 and -0.000002 radians. The new focal length is 5.00001 m.

The deformation patterns of the two cases before fitting are shown in Figure 10. Figure 10-a is the pattern when the x- component of the gravitational force is applied. In this figure, larger deformations of the surface occur at the edge of the dish and the absolute value of the deformation is very small (maximum deformation is 35 microns). Therefore the rms error in this direction is very small as well. This agrees very well with the theoretical analysis provided in this memo. The double layer truss structure indeed acts as a shell because the force components normal to the surface are nearly uniform in the center part of the dish. Figure 10-b is the

deflection pattern when the y-component of the gravitation force is applied. In this figure, the absolute deformations of the structure are symmetrical about the OXZ plane. However, the directions of the deformations in the two parts are opposite. Although the maximum deflection is about 120 microns (this is much larger than that in Figure 10-a), the rms deviation from the best-fit paraboloid is still very small. In both directions, the gravitationally induced rms errors are better than most symmetrical antenna structures, including submillimeter antennas.

4.4 Other aspects of the structure.

The secondary mirror support structure is designed to have three main supporting beams as shown in Figure 9. All these beams are supported from the base of the bearing disk. The main support of the secondary mirror is by the center beam, which is also a space truss structure itself. Between the truss structure and the slant bearing, a special design will be provided to reduce thermal effects. Both the slant bearing and the azimuth bearings are identical in size and shape. Both bearings may be formed by two layers of bearings arranged in a conical shape (ref. Figure 6). The top layer bearing has a smaller diameter and the bottom layer bearing has a larger diameter. This arrangement increases the bearing accuracy and provides more space for a third mirror or receiver. The base and the middle slant cabin are thermally insulated with air conditioning to maintain a constant temperature. The base legs are above the ground to ease the transportation problem. The truss structure should use highly reflecting protection and remain as an open structure.

5.0 Advantages and shortcomings of an offset slant axis antenna.

Compared with the classical Cassegrain arrangement and other designs, the offset slant axis antenna has the following advantages:

i) The aperture efficiency, the sidelobe and ground pickup are all improved.
ii) Because we are not concerned about subreflector blockage, the options for low-frequency feeds and for focal-plane arrays are greater.
iii) The counterweight for the backup structure is removed.
iv) There is plenty of space for the secondary mirror supporting structure; the stiffness can be improved without aperture efficiency loss. The structure natural frequency should be the same as or even better than that of the slant axis symmetric design.
v) There are more mounting options for receivers, and there is more space for cryogenic equipment next to the receiver. The flexing of cryogenic lines is eliminated.
vi) There is a significant saving in the overall structural weight compared with the classical Cassegrain design. The corresponding cost will be reduced.
vii) Since the force applied to the backup structure is near to the truss plane, the rms distortion of the surface nodes will be less sensitive to the details of the truss structure. The backup structure manufacture and assembly is less critical.
viii) The effect of wind on pointing is reduced. The wind direction is never normal to the antenna surface, to first order the wind load is balanced, and the drive motors never compete directly with wind forces.

ix) The main truss structure is simple in shape. There are repeated patterns which reduce the number of the truss member types and node joint types. It is easier for mass production.

Compared with the classical Cassegrain design, the offset slant axis antenna offers many advantages. For the mmA array with 40 antenna dishes, the gain from the reduced blockage of the offset antennas is equivalent to the extra collecting area of four complete antennas.

Possible shortcomings of this offset slant axis design are:

i) There are more panels and panel types for each antenna than for a symmetrical antenna structure. However, this design provides higher efficiency. For the mmA array with 40 antennas the greater number of panel types will add little additional cost.
ii) It is difficult to apply an on-axis encoder to the slant axis.
iii) The polarization characteristics[16] of this Open Cassegrain design may be inferior to a conventional symmetric design. A mmA memo in preparation by Peter Napier will study this aspect of the antenna performance [17].

Another area of future study is how closely the antennas can be positioned for the compact array configuration.

6.0 Conclusion.

The advantages of the aperture efficiency and clean beam pattern make the offset design an ideal candidate for many large and precise antennas. In the past, this has not been possible because the optimization of such an unsymmetrical structure is extremely difficult. However, by combining the advantages of the slant axis mounting structure and the double layer space truss design, it is now possible to design an offset antenna with very high homologous performance. This is a significant advance in the design philosophy for large and precise antennas beyond the original development of the homology principle by Von Hoerner in the 1960s[13]. The principle of the design described in this memo can also be used for other larger and more precise antenna projects.

The new design for the mmA antennas is a logical development of the slant axis symmetrical structure, which was first proposed for the mmA by J. Payne and J. Lamb. The offset slant axis design has been discussed for lower frequencies by Denkmann et. al.[12],[14]. The author express his thanks to R. Brown, D. Emerson and J. Payne for encouragement and many discussions. Thanks are due to P. Napier for comments on the polarization characteristics of the antenna.

References.

[1] Cheng, J., Slanted-axis antenna design I, mmA antenna memo. No. 12, 1993.
[2] Cheng, J., Slanted-axis antenna design II, mmA antenna memo. No. 16, 1994.
[3] Cheng. J., A slant-axis antenna for mmA: Computer simulation results of fast switching,

mmA antenna memo. No. 17, 1994.
[4] Lawrence, C.R., Hetbig, T., and Readhead, A.C.S., Reduction of ground spillover in the Owens Valley 5.5m telescope, Proceedings of the IEEE, 1993.
[5] Lamb, J., Proposed surface error budget for mmA antennas, mmA antenna memo. No.11, 1993.
[6] Cheng, J, Steerable parabolic antenna design, Ph.D. thesis, University College Cardiff, U.K. 1984.
[7] Payne, J., Pointing and surface control of GBT, GBT memo. No. 36, 1990.
[8] Niordson, F.I., Shell theory, North-holland, New York, 1985.
[9] Makowski, Z.S., Review of the development of various types of double-layer grids, from 'Analysis, design and construction of double layer grids', Applied science publishers Ltd., London, 1981.
[10] Timoshenko, S., Strength of materials, Van Nostand reinhold company, New York, 1958.
[11] Cook, J.S., Elam, E.M. and Zucker, H., The open Cassegrain antenna: part I. Electromagnetic design and analysis, The Bell system technical journal, Sept, 1965.
[12] Denkmann, W.J. et. al., The open Cassegrain antenna: part II. Structural and mechanical evaluation, The Bell system technical journal, Sept. 1965.
[13] Von Hoerner, S., Homologous deformation of tiltable telescopes, J. Struc. Div. Proc., ASCE, Vol 95, ST-6, 1139-1152, 1967.
[14] Lorrain, P. and Corson, D., Electromagnetic fields and waves, W.H. Freeman and Company, San Francisco, 1962.
[15] Butterworth, J.W., Analysis, design and development of double-layer grid, ed. Makowski, Applied science pubishers, London, 1981
[16] Fourikis, N., A parametric study of the constraints related to Gregorian/Cassegrain offset reflectors having negligible cross polarization, IEEE trans. on antennas and propagation, Vol. 36, No. 1, 144-147, 1988.
[17] Napier, P., Polarization Properties of an Open Cassegrain Antenna, mmA antenna memo, in preparation (1994).

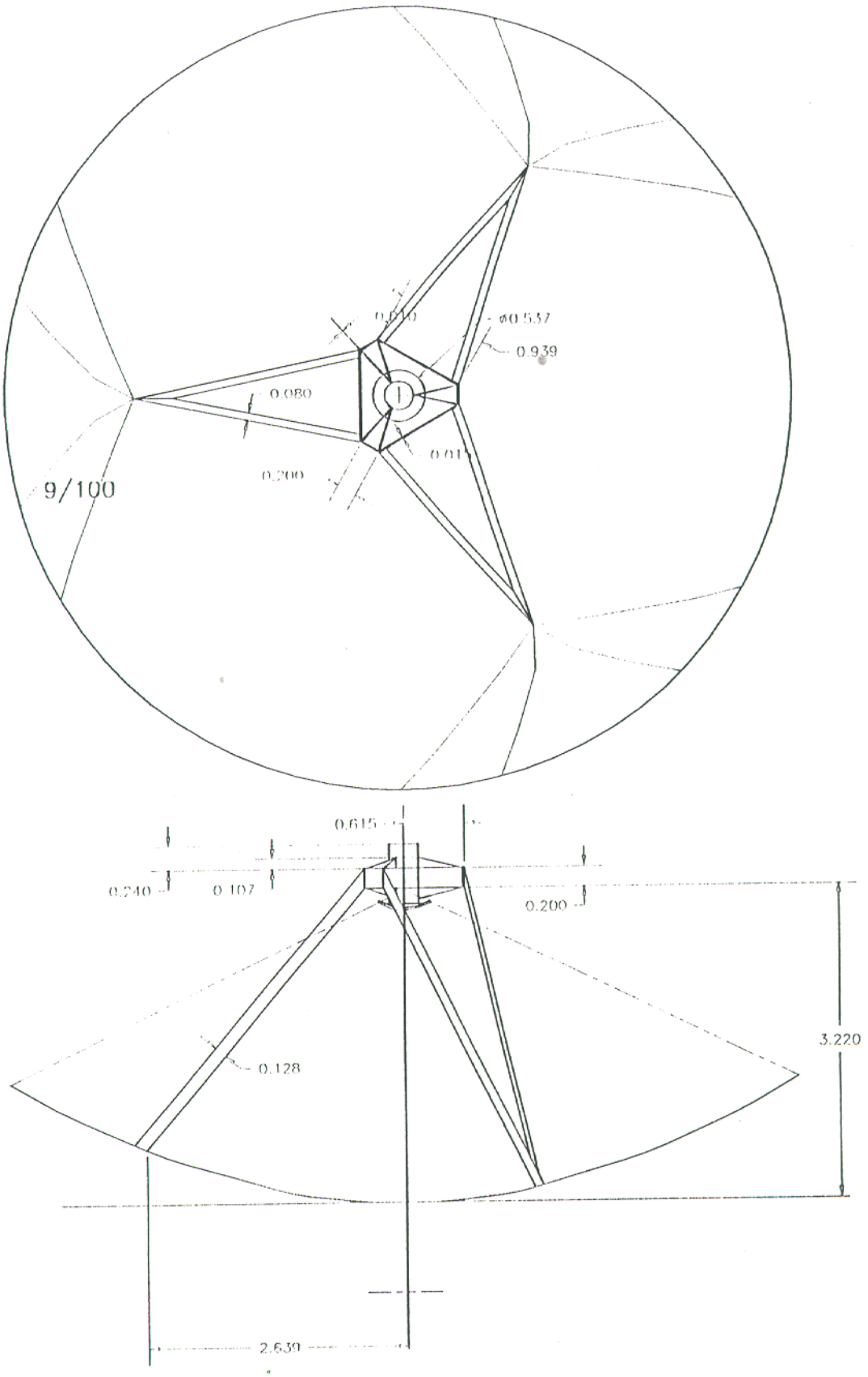

Figure 1 Indirect aperture blockage caused by the secondary mirror support structure of a symmetrical antenna.

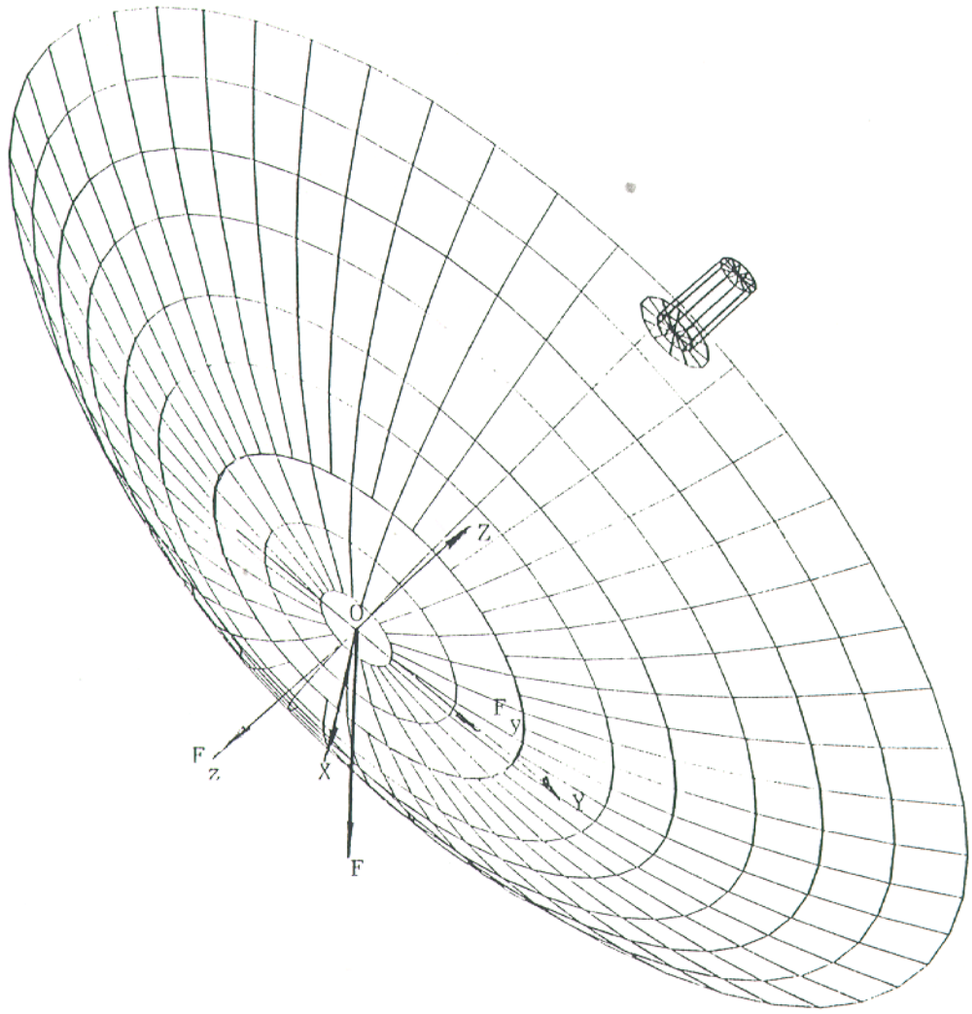

Figure 2-a Force vectors of altazimuth mounted antenna;

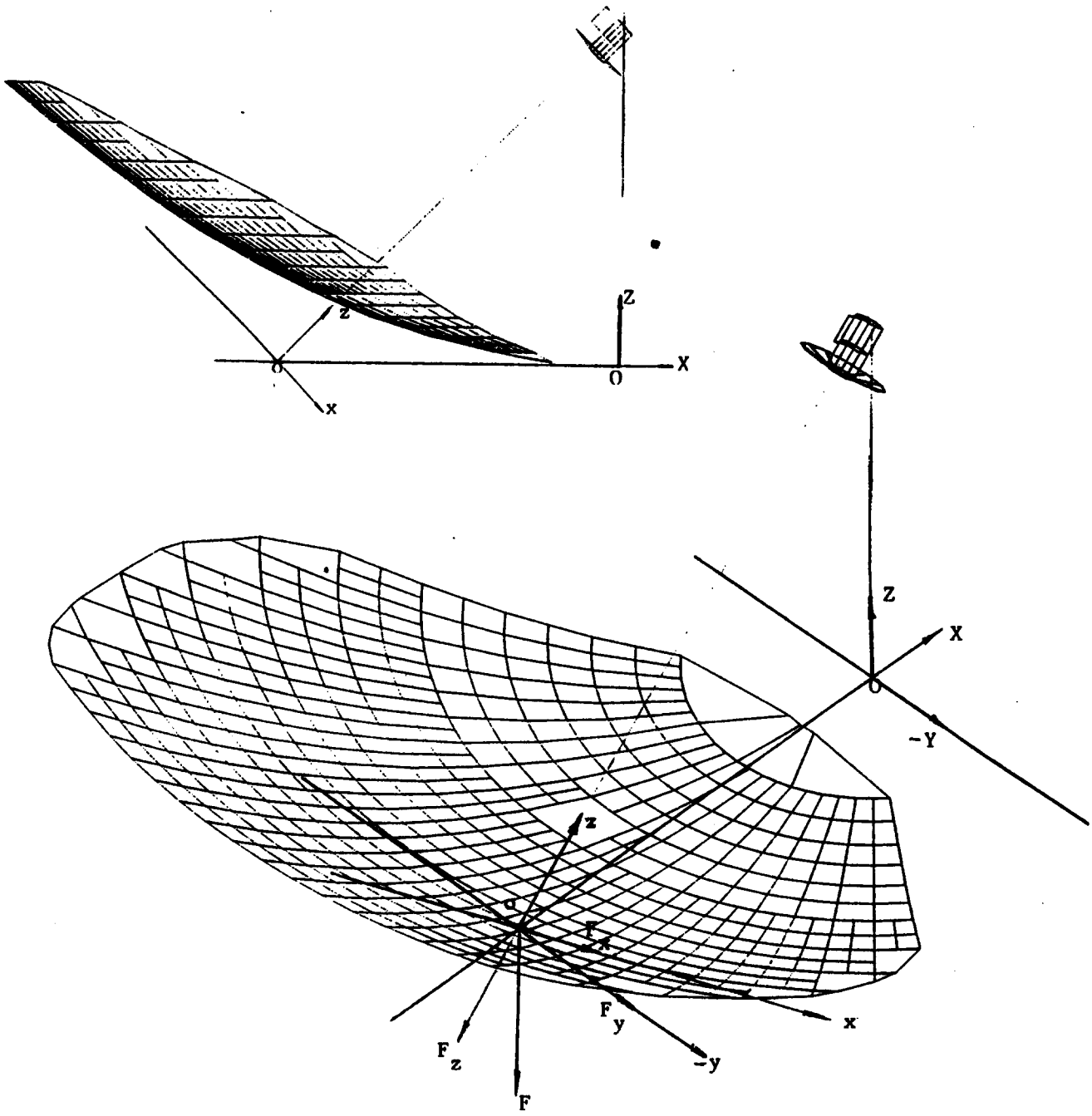

Figure 2-b Force vectors of slant axis mounting antenna.

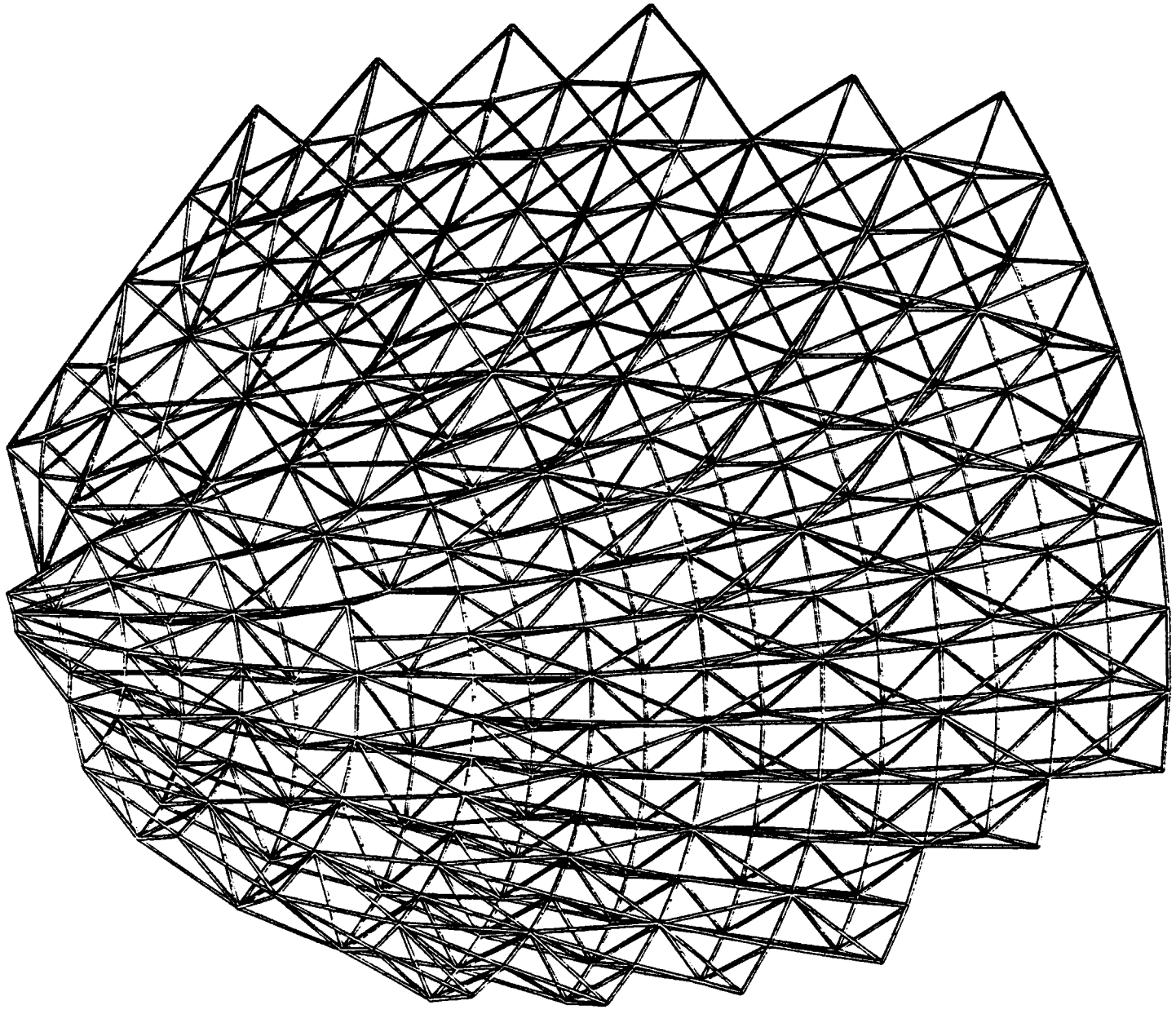

Figure 3 View of the main truss structure proposed for the offset mmA antenna.

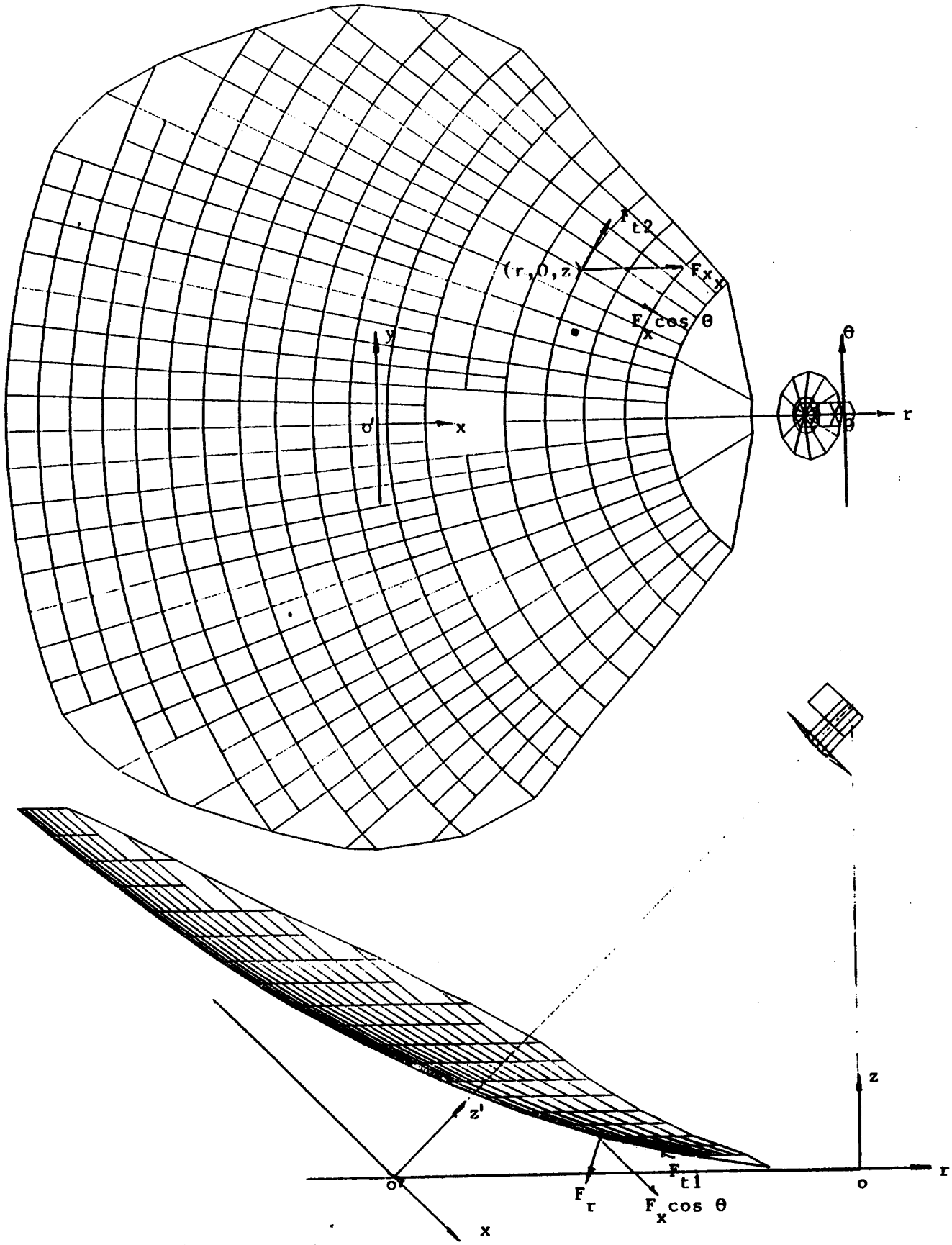

Figure 4 Decomposition of F_x in the local coordinate system.

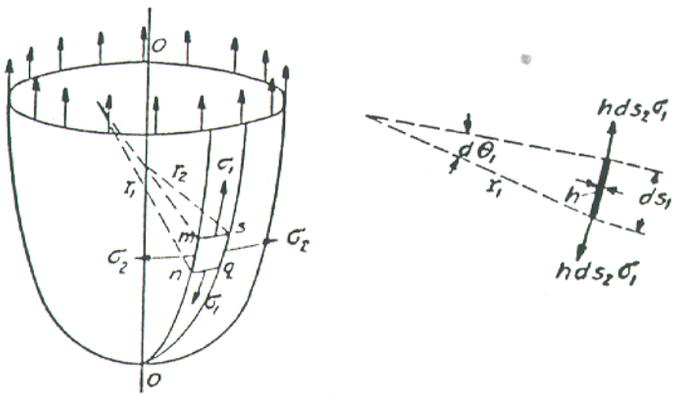

Figure 5-a The relationship of the shell pressure and stresses produced.

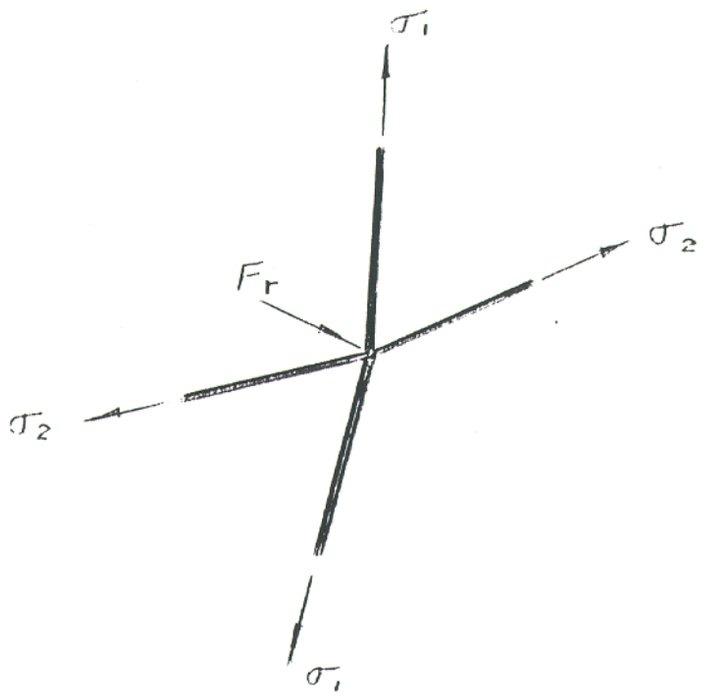

Figure 5-b The shell like truss structure with uniform forces on the joints.

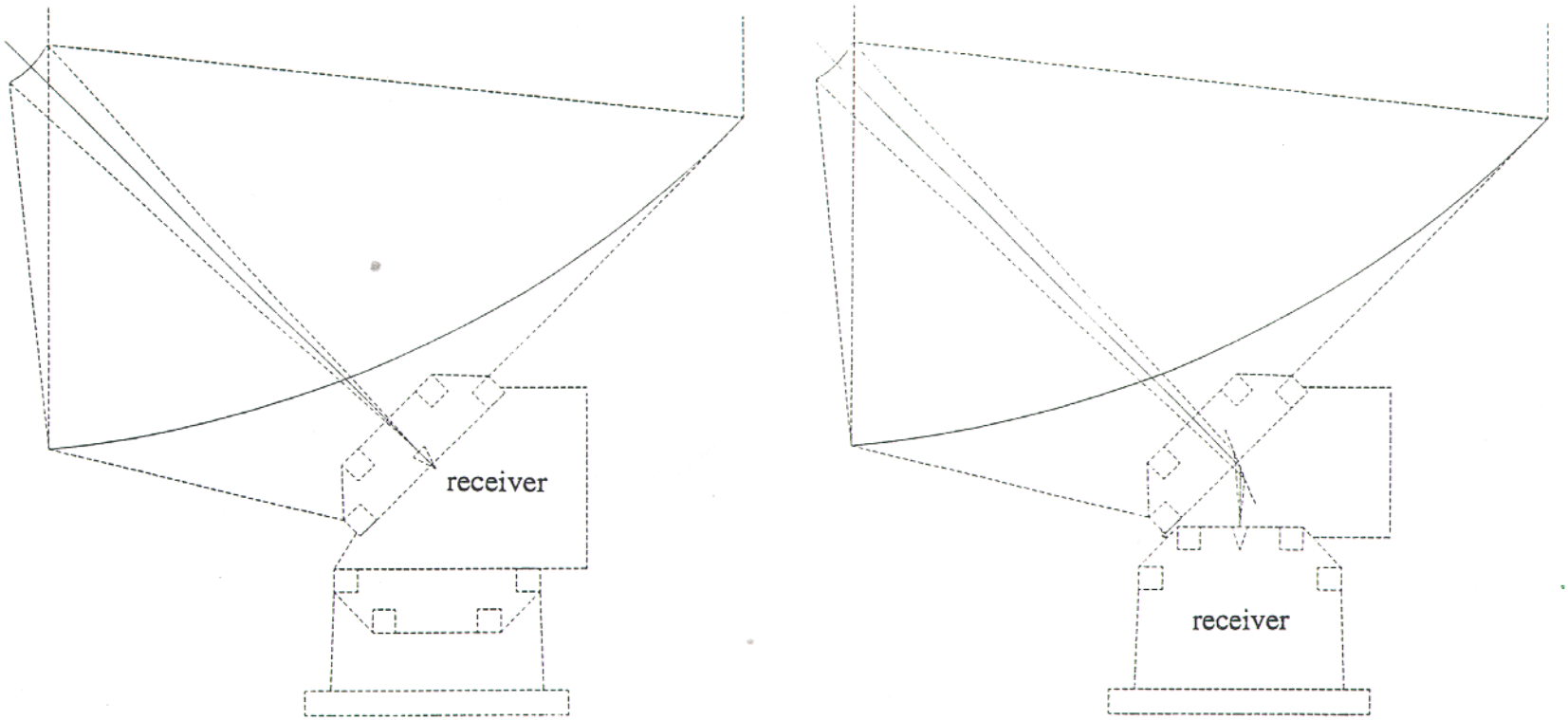

Figure 6 Possible optical arrangements of the offset slant axis antenna.
a) the receiver is located at receiver cabin; b) the receiver is located at the base.

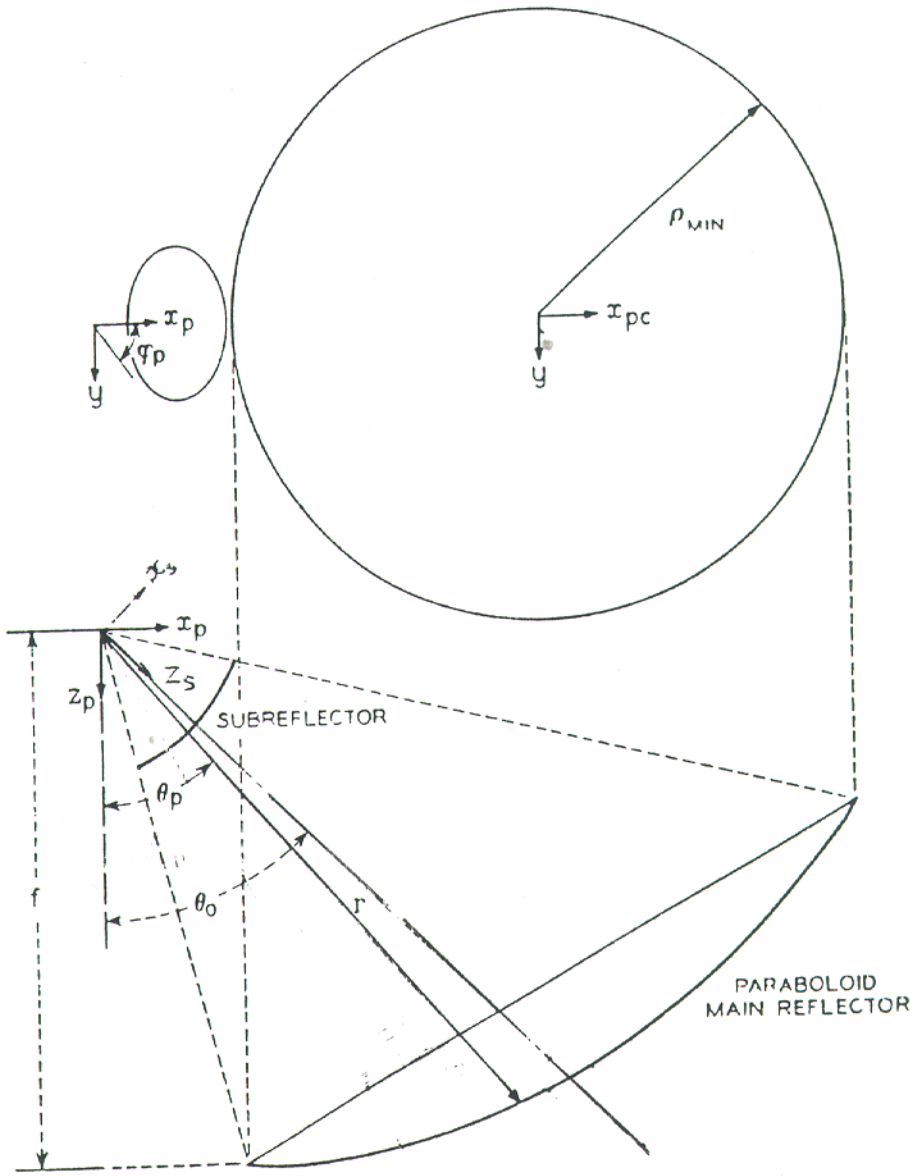

Figure 7 Projected view of the optics and its related coordinate systems.

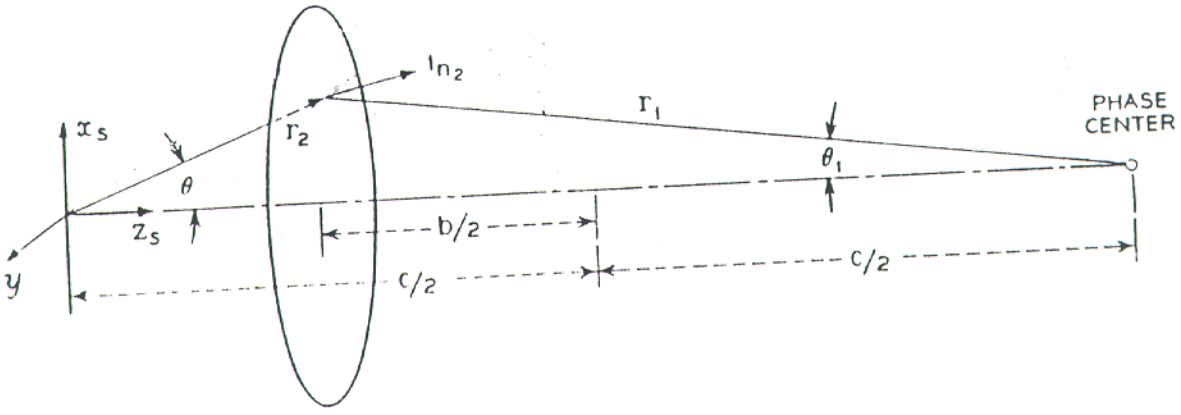

Figure 8 The geometry of the secondary mirror surface.

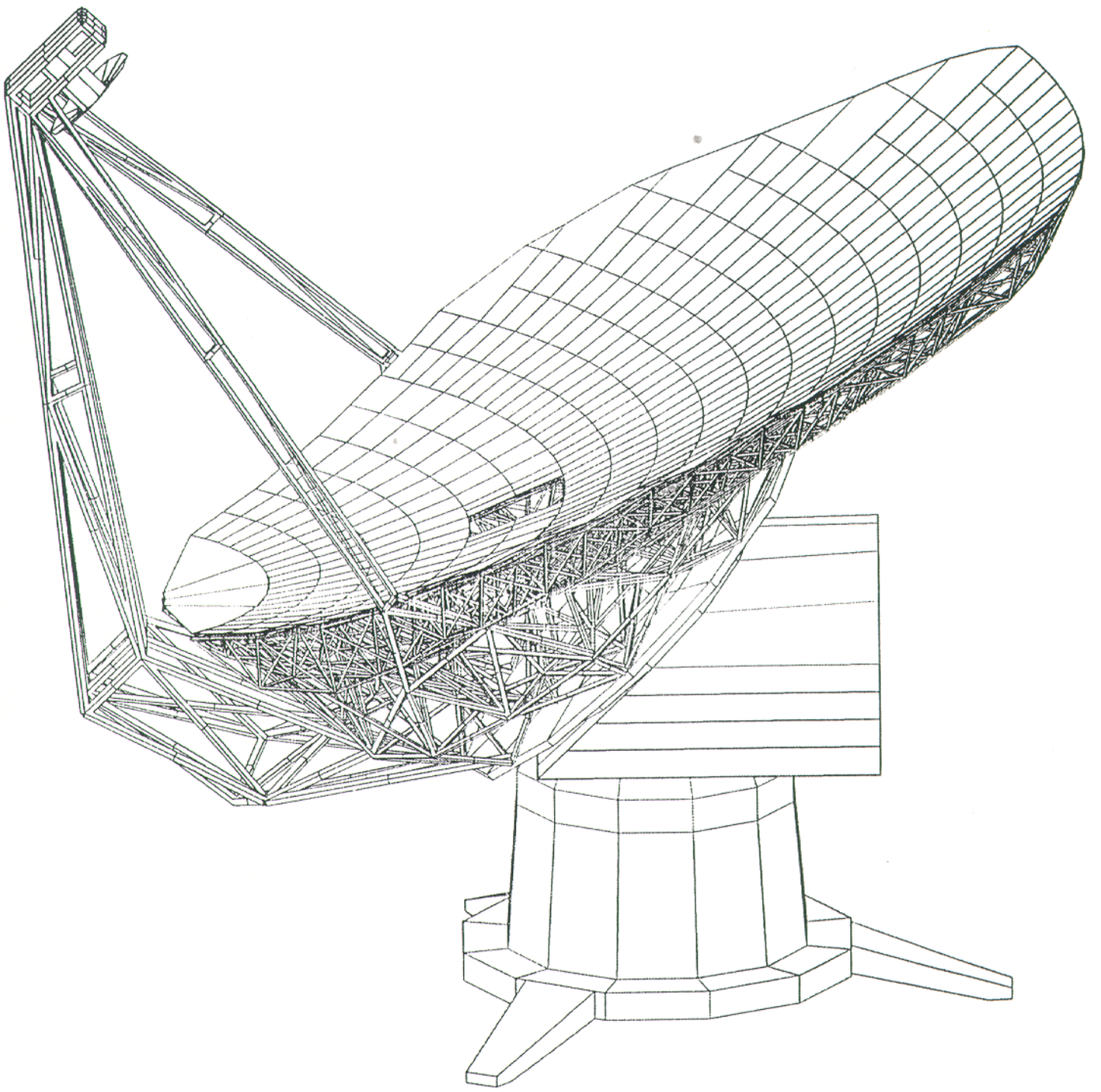

Figure 9 Perspective view of the proposed mmA offset slant axis antenna.

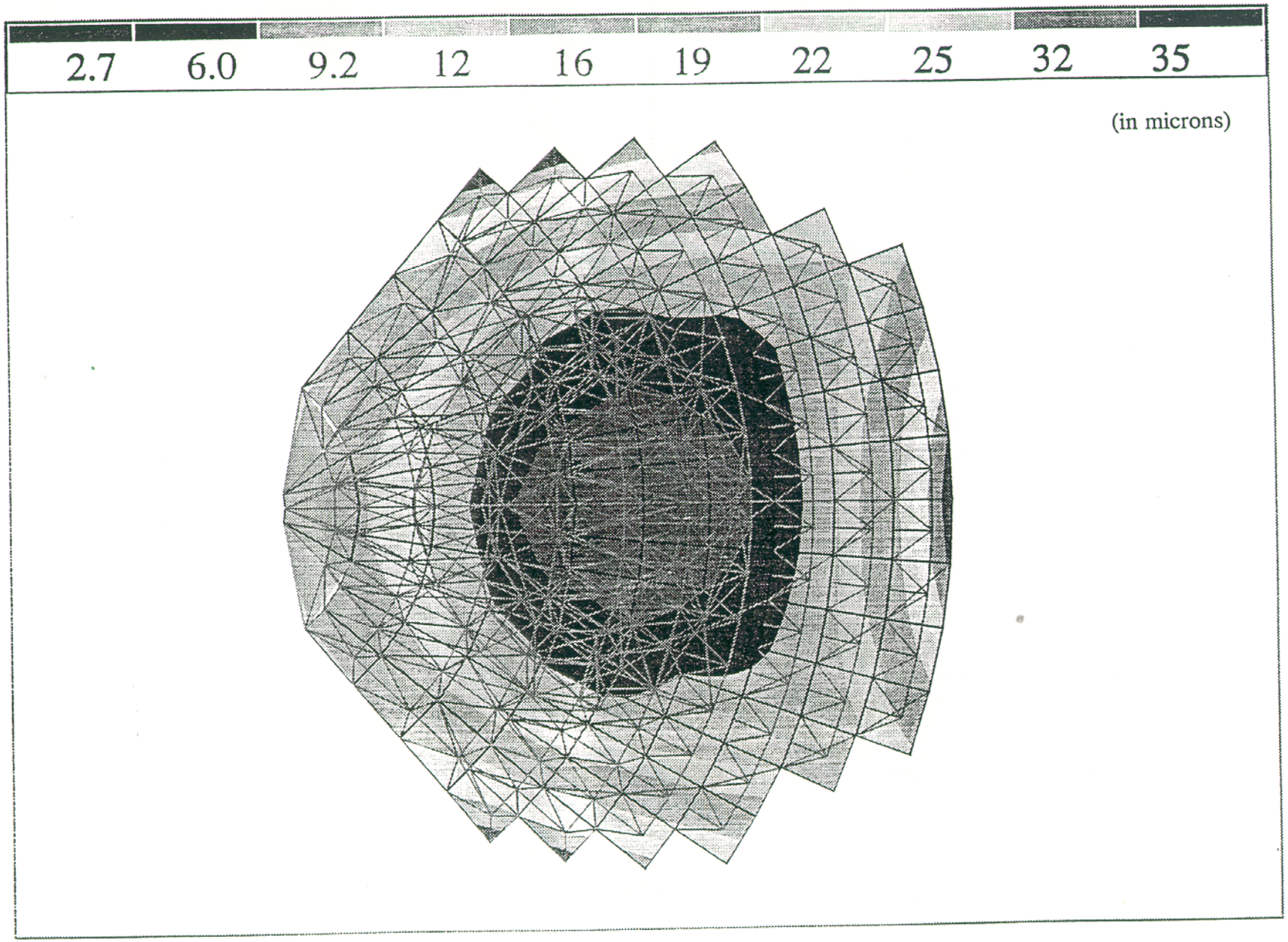

Figure 10-a The deformation pattern under the gravitation force component F_x.

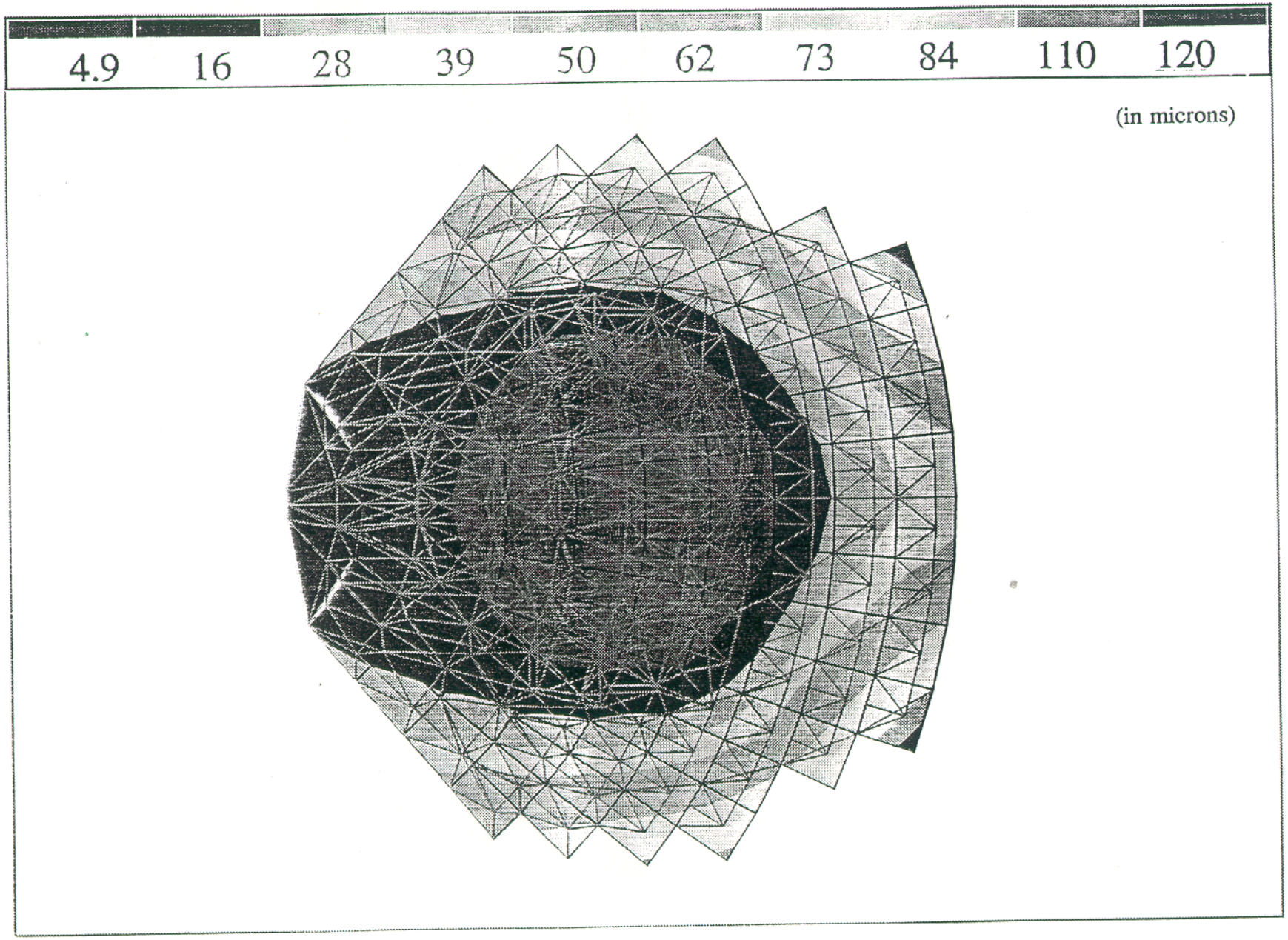

Figure 10-b The deformation pattern under the gravitation force component F_y.